# Diel cycle of lanthanide-dependent methylotrophy by TMED127/Methylaequorales bacteria in oligotrophic surface seawater

Jennifer B. Glass[1*], Leilani N. Warters[1], Abdulaziz M. Alajlan[1]

[1]School of Earth and Atmospheric Sciences, Georgia Institute of Technology, Atlanta, GA, USA

*Corresponding author: Jennifer.Glass@eas.gatech.edu

**Abstract**

Methanol, the simplest alcohol, has long been recognized as a key energy and carbon source for soil and plant-associated bacteria and fungi, and is increasingly recognized as an important substrate for marine bacteria. Lanthanide-dependent methanol dehydrogenases (encoded by the gene *xoxF*) are now recognized as the key catalysts for methylotrophy in many environments, yet the identity of the most transcriptionally active methylotrophs in open ocean waters ("Clade X") has remained elusive. Here we show that "Clade X" methylotrophs belong to the deep-branching alphaproteobacterial order TMED127, which we propose be renamed 'Methylaequorales'; 'methyl' for 'methylotrophic metabolism' and 'aequor' for 'ocean surface', as these bacteria are most transcriptionally active near the sea surface. TMED127/Methylaequorales are present in surface waters of tropical and subtropical oceans throughout the global ocean. They have small, streamlined genomes (~1.5 Mb), and appear to be obligate methylotrophs that use the serine cycle for carbon assimilation. They display a diel pattern of *xoxF5* and glucose dehydrogenase (*gdh*) transcription, peaking in the late afternoon, in oligotrophic surface water of the Sargasso Sea. Several other highly transcribed genes of unknown function had no homologs outside of TMED127/Methylaequorales genomes. Our findings illuminate an overlooked marine methylotrophic bacterium and predict a diel cycle of methanol production in surface seawater by an unknown pathway.

**Importance**

Methanol metabolism is increasingly recognized as an important process in the marine carbon cycle, yet the identity and metabolism of the microorganisms mediating methylotrophy in the open ocean have remained unknown. This study reveals that bacteria in the TMED127 order of

Alphaproteobacteria, proposed new name of "Methylaequorales", abundantly transcribe the key gene for lanthanide-dependent methylotrophy in oligotrophic surface waters of the world's oceans. TMED127/Methylaequorales likely require methanol as a carbon and energy source and display a diel pattern of transcription of key genes for methylotrophy that peaks in the late afternoon. These findings motivate future studies on the mechanisms of methanol production in surface seawater.

## Introduction

Methanol ($CH_3OH$) is a simple alcohol that is used by methylotrophic bacteria as an energy and carbon source (1, 2). The first step of bacterial methylotrophy, oxidation of methanol to formaldehyde, is mediated the periplasmic enzyme pyrrolo-quinoline quinone (PQQ) methanol dehydrogenase, which requires either calcium or a light lanthanide elements (lanthanum, cerium, praseodymium, and neodymium) as its cofactor (3). Lanthanide-dependent methanol dehydrogenases are encoded by the gene *xoxF* and calcium-dependent methanol dehydrogenases are encoded by the gene *mxaF*. Formaldehyde produced by methanol dehydrogenase is then further oxidized to yield energy for cellular growth and/or assimilated into cellular carbon via the ribulose monophosphate cycle or the serine cycle (4).

Methylotrophy appears to be widespread in terrestrial and marine ecosystems. Plants make methanol from cell wall pectins using pectin methylesterase (5), and terrestrial plant-associated methylotrophic bacteria have been extensively studied for their agricultural importance (6). Methanol is also produced by marine phytoplankton via unknown mechanism(s) (7, 8) and can also be produced abiotically by photodegradation of methoxy aromatic groups in lignin (9) or reaction of methyl peroxy radical with hydroxyl radicals (10). Some marine bacteria secrete pectin methyltransferases, possibly producing methanol as a byproduct (11-13). Most methanol

emitted to the atmosphere is rapidly deposited back to the ocean surface (14-16), where it is rapidly consumed by bacteria for energy and, to a lesser degree, for carbon assimilation (17-21).

Although calcium is nine orders of magnitude more abundant than lanthanides in seawater, marine microbial methanol oxidation is primarily lanthanide dependent, based on the prevalence and transcriptional activity of *xoxF* compared to *mxaF* (22). The dominant types of *xoxF* in most natural environments are *xoxF5*, found in many orders of Alpha- and Gammaproteobacteria, and *xoxF4*, found in Methylophilaceae (23, 24). Selective drawdown of light lanthanides relative to heavy lanthanides in seawater is associated with biological activity (25-27). In coastal waters, methylotrophic bacteria are dominated by Methylophilaceae (also known as OM43; 28, 29-34), which possess *xoxF4*, and Methylophagaceae, which possess both *xoxF5* and *mxaF* (21, 35-37). Omics studies have revealed a much broader diversity of marine bacteria with the capacity for lanthanide-based methylotrophy than previously realized (24, 38-41). A recent study reported an unidentified alphaproteobacterial "Clade X" of *xoxF5* genes as having highest transcriptional activity in Tara Oceans seawater samples (22). Here we investigated the identity, predicted metabolism, and transcriptional activity of methylotrophic bacteria in oligotrophic waters representative of the vast majority of the ocean's surface to resolve the identity and metabolism of the elusive "Clade X" methylotroph.

## Results

***Most highly transcribed xoxF5 genes in oligotrophic surface seawater belong to the alphaproteobacterial order TMED127.*** RNA-Seq datasets in the Department of Energy (DOE) Joint Genome Institute Integrated Microbial Genomes and Microbiomes (JGI IMG/M) database (42) were searched for PQQ-dependent methanol dehydrogenases (see Materials and Methods

for details). We found extremely high transcription of lanthanide-dependent methanol dehydrogenase *xoxF5* genes (up to 2056 RPKM) in oligotrophic surface seawater from three different ocean basins (North Atlantic, South Atlantic, and Indian Ocean (39, 43-45); **Table S1)**. In a dataset from the Bermuda Atlantic Time-series Study (BATS; Sargasso Sea, North Atlantic Ocean) with free-living (SX) and particulate (LSF) size fractions, *xoxF5* transcripts were almost exclusively present in free-living fractions (**Table S1)**, suggesting that active methylotrophs are free living rather than particle associated. The most highly transcribed *xoxF5* genes had high identity (93-100%) to genes from genus GCA-002690875 and GCA-2691245 of the uncultured marine alphaproteobacterial order TMED127 (GTDB taxonomy; 46), previously known as "Ricksettsiales" in NCBI taxonomy **(Fig. 1A; Table S1)**. Multiple identical full-length sequences in TMED127 genus GCA-2691245 were recovered **(Table S1)**, motivating further analysis of this genus (see below).

TMED127 *xoxF5* genes form a monophyletic clade with other Alphaproteobacteria *xoxF5* genes from the orders UBA8558 and UBA11136 that are transcribed in deeper seawater samples (10-150 RPKM; **Fig. 1A; Table S1**). BLAST searches of metatranscriptomes from the Eastern Tropical North Pacific oxygen deficient zone (47) revealed that UBA11136 *xoxF5* transcripts are abundantly transcribed (up to 550 RPKM) in anoxic waters **(Table S2)**, supporting the hypothesis that UBA11136 oxidizes methanol in oxygen deficient zones (48). Other Alphaproteobacteria (GCA-002720895) and Gammaproteobacteria (Burkholderiales (genus UBA7377) and UBA4486) also transcribed *xoxF5* genes in globally distributed samples and across a range of depths (10-500 RPKM; **Fig. 1A; Table S1**), consistent with previous reports (38, 41). As predicted, Methylophilaceae/OM43 *xoxF4* transcripts (1-350 RPKM) were present in coastal waters **(Fig. 1A; Table S1)**.

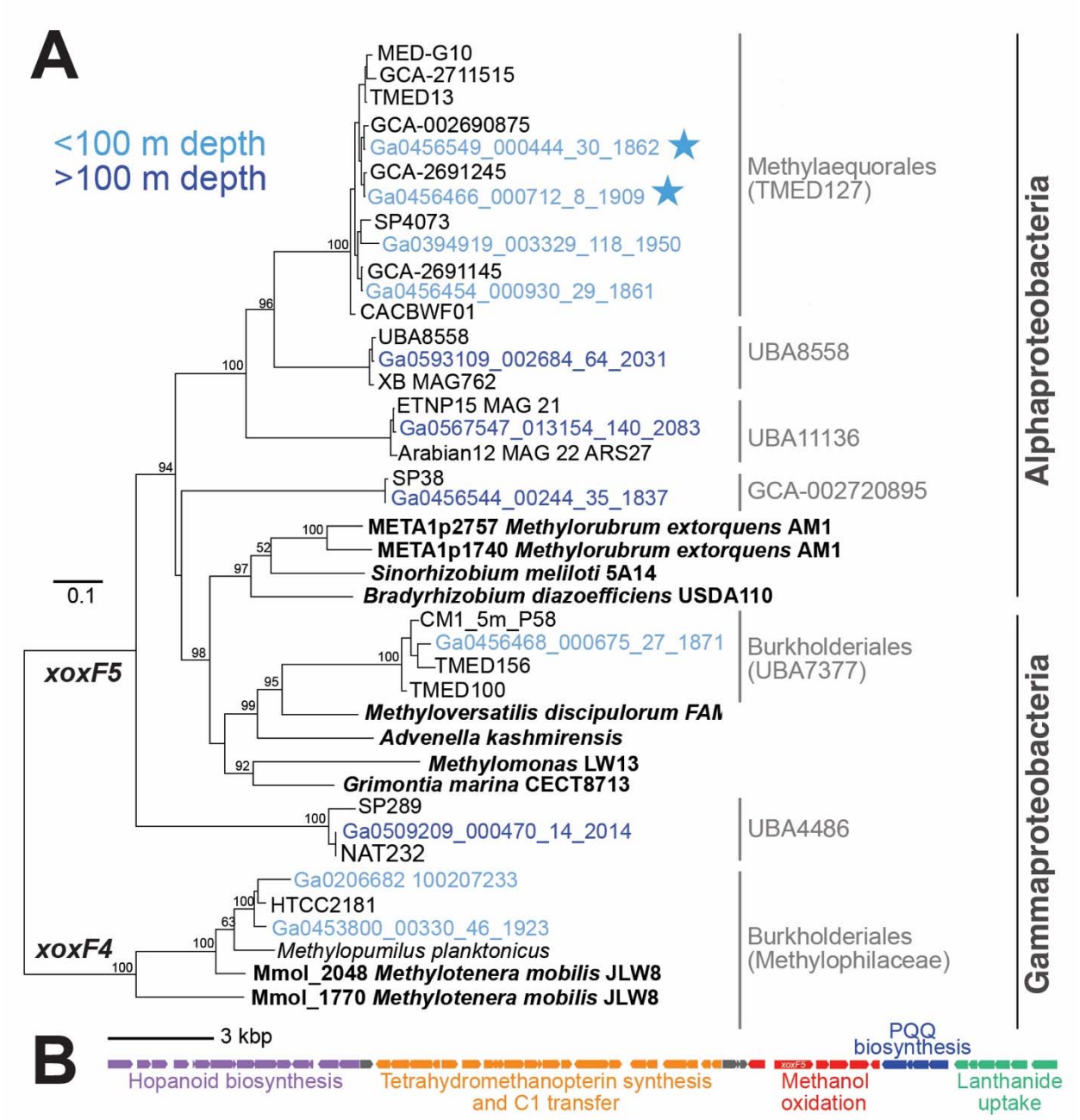


**Figure 1. Lanthanide-dependent methanol dehydrogenase (XoxF) phylogeny and "methylotrophy island" in TMED127 genomes.** (A) Maximum likelihood phylogenetic tree of PQQ-methanol dehydrogenases XoxF5 sequences, with XoxF4 sequences as outgroup. Sample depths are colored (light blue: 0-100 m depth; dark blue: >100 m depth). All JGI IMG sequences (beginning with "Ga") are available in **Table S1**, and those with >100 RPKM in any sample JGI IMG are on the phylogeny. Classes are in dark gray. Orders containing highly transcribed marine JGI IMG samples are labeled in light gray according to GTDB taxonomy. TMED127 nodes are labeled by genera; all other nodes are labeled by SAG/MAG isolate name or species name. The stars mark the JGI IMG seawater samples with highest transcription from the Sargasso Sea. Sequences encoding biochemically characterized enzymes (bold) are from refs. (23, 24, 49). The

two Burkholderiales clades are designated by family (Methylophilaceae) and genus (UBA7377). (B) "Methylotrophy island" (~45 kbp) in TMED127 genomes (drawn based on isolate CM1_5m.P40), with the following modules: hopanoid biosynthesis (CM15mP40_03190-03050), tetrahydromethanopterin synthesis and C1 transfer (CM15mP40_03030-02810), methanol oxidation (CM15mP40_02770-02720), PQQ biosynthesis (CM15mP40_02710-02680), and lanthanide uptake (CM15mP40_02670-02620). Gray indicates hypothetical proteins.

***TMED127 genomes are small and contain "methylotrophy island".*** There are 64 TMED127 SAG/MAGs in GTDB (RS207 and RS226), originating from seawater samples of the Atlantic Ocean, Pacific Ocean, Mediterranean Sea, Red Sea, and Brisbane River **(Table S3)**. These include three MAGs comprising "Clade X" in ref. (22): MED715, MED652, and MED657 (**Table S3)**. TMED127 SAG/MAGs are small (~1.5 Mb estimated complete size) and contain a ~45 kbp "methylotrophy island" with genes for methanol oxidation, tetrahydromethanopterin synthesis and C1 transfer, lanthanide uptake (*lutABEFCG* (50)), and pyrroloquinoline quinone (PQQ) biosynthesis (**Fig. 1B).** Upstream of the "methylotrophy island" is a gene cluster encoding the hopanoid biosynthetic pathway implicated in structural ordering of the outer membrane (51, 52). We identified the "methylotrophy island" in 44 of the 64 TMED127 SAG/MAGs, spanning eight genera **(Table S3)**, including the three MAGs previously shown to comprise "Clade X", suggesting that the "methylotrophy island" is present throughout the TMED127 order. Other TMED127 SAG/MAGs appeared to have the same gene synteny but had truncated *xoxF5*-containing contigs.

***Diel transcriptional rhythm of methanol and glucose dehydrogenases in TMED127.*** A previous metatranscriptomic time series at BATS found that ~10% of all genes had diel transcriptional patterns (44). To assess transcription of TMED127 genes, we mapped transcripts from surface seawater (5 m depth) from the previous study, sampled every 4 hours over 5 days **(Table S4)**, to most complete TMED127 SAG from genus GCA-2691245 (AG-892-F10; estimated 90% completeness; 0.01% contamination (53); **Fig. 1A; Table S1**). Throughout the

time series, *xoxF5* was consistently the most abundant transcript, comprising 16 to 57% (1.6 to 5.7 x $10^5$ TPM) of AG-892-F10 transcripts **(Table S5)**. The *xoxF5* gene displayed a diel transcriptional cycle, consistently peaking in the late afternoon (16:00-20:00; **Fig. 2**). A PQQ-dependent glucose dehydrogenase (*gdh*), which likely produces the lanthanide chelator D-glucono-1,5-lactone, showed the same transcriptional pattern at roughly an order of magnitude lower abundance **(Fig. 2; Table S5)**. Five other genes were transcribed at >$10^4$ TPM but not did not show a temporal pattern; these included proteorhodopsin, two hypothetical proteins (AG-892-F10.CDS.256 and AG-892-F10.CDS.257), the phosphate ABC transport substrate-binding protein (*pstS*), and a DoxX-like family protein (**Table S5)**. Homologs of AG-892-F10.CDS.256 and AG-892-F10.CDS.257 (34% lysine), were only present in other TMED127 SAGs/MAGs, whereas the DoxX-like integral membrane family protein had homologs in other marine Alphaproteobacteria and Methylophilacaeae/OM43.

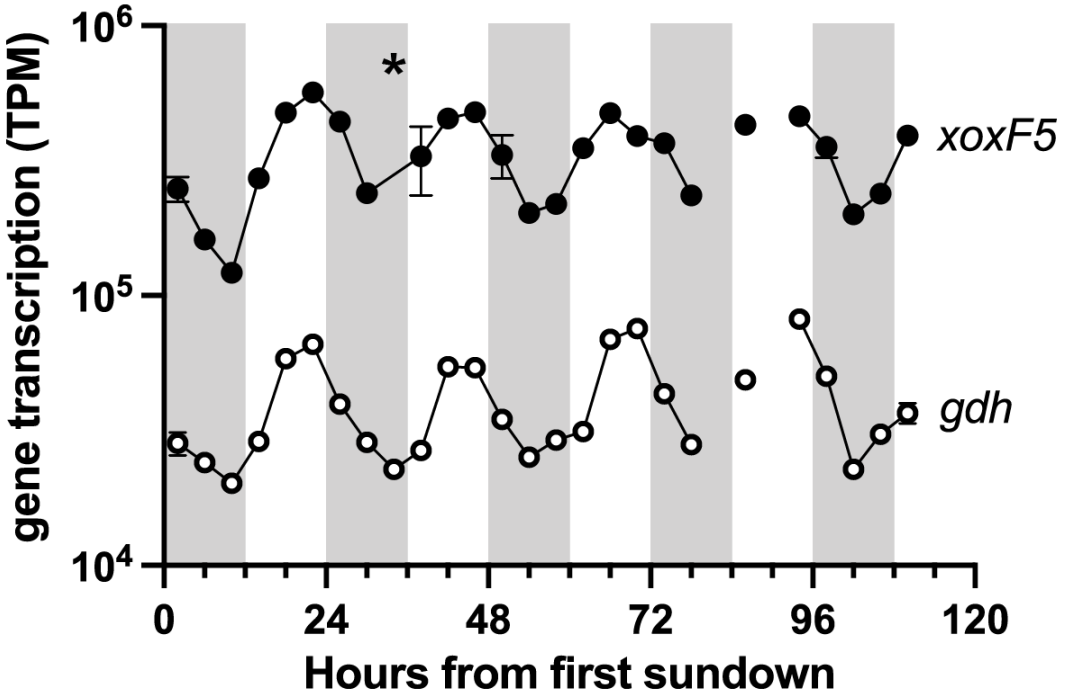


**Figure 2. Diel transcription of TMED127 lanthanide-dependent methanol dehydrogenase (*xoxF5*) and glucose dehydrogenase (*gdh*) at Bermuda Atlantic Time-series Study (BATS)**

**site, Sargasso Sea, North Atlantic Ocean.** The asterisk represents a single anonymously high sample. Error bars (standard deviation) are shown for the nine time points with multiple metatranscriptomes. Missing lines are due to lack of samples for two timepoints.

***TMED127 are likely obligate methylotrophs.*** Genomic analysis suggests that TMED127 are obligate methylotrophs. TMED127's core methylotrophic modules match those of the well-studied plant-associated facultative methylotroph *Methylorubrum extorquens* AM1 (54, 55); roughly two-thirds (956/1535) of AG-892-F10's genes have homologs in AM1 **(Tables S5)**. Based on extensive previous studies of AM1 metabolism (56, 57), we predict that TMED127 uses the same methylotrophy pathways: after methanol oxidation via XoxF, formaldehyde is oxidized to formate via the tetrahydromethanopterin C1 transfer pathway, which is then either oxidized to $CO_2$ by tungsten-containing formate dehydrogenase for regeneration of NAD(P)H or assimilated into biomass via the serine and ethylmalonyl-CoA pathways **(Fig. 3; Table S5)**. TMED127 genes without AM1 homologs include several genes common in marine proteobacteria (e.g., proteorhodopsin for light-driven proton pumping and nickel-dependent superoxide dismutase **(Fig. 3))**. While TMED127's small (~1.5 Mb) genome has only one copy of most key functional genes, AM1's large (6.9 Mb) genome has multiple copies of many key functional genes. AM1 also has a full TCA cycle, enabling its growth on multiple-carbon compounds. Although we cannot be certain of gene absence in incomplete genomes, none of the 64 SAGs/MAGs was found to possess the 2-oxoglutarate dehydrogenase complex, suggesting that they have incomplete TCA cycles characteristic of obligate methylotrophs (58).

***Description of proposed TMED127 names.*** We propose that the species studied in the present study (AG-892-F10, genus GCA-2691245) be named *Methylaequorum cenaphilum* gen. nov., sp. nov. : Me.thy.lae.quo'rum N.L. neut. n. *methyl*, pertaining to the methyl group; L. neut. n. *aequor*, surface of the sea; N.L. neut. n. *Methylaequorum*, methyl (group oxidizing) organism

[of the] sea surface; ce.na.phi'lum L. fem. n. *cena*, the principal meal of the day in ancient Roman culture, originally taken in the afternoon; N.L. masc. adj. suff. *-philus*, loving; N.L. neut. adj. *cenaphilum*, late afternoon meal loving. At the family level, Me.thy.lae.quo.ra'ce.ae. N.L. neut. n. *Methylaequorum*, referring to the type genus Methylaequorum; *-aceae*, ending to denote a family; N.L. fem. pl. n. *Methylaequoraceae*, the Methylaequorum family. At the order level, Me.thy.lae.quo.ra'les N.L. neut. n. *Methylaequorum*, referring to the type genus Methylaequorum; *-ales*, ending to denote an order; N.L. fem. pl. n. *Methylaequorales*, the Methylaequorum order.

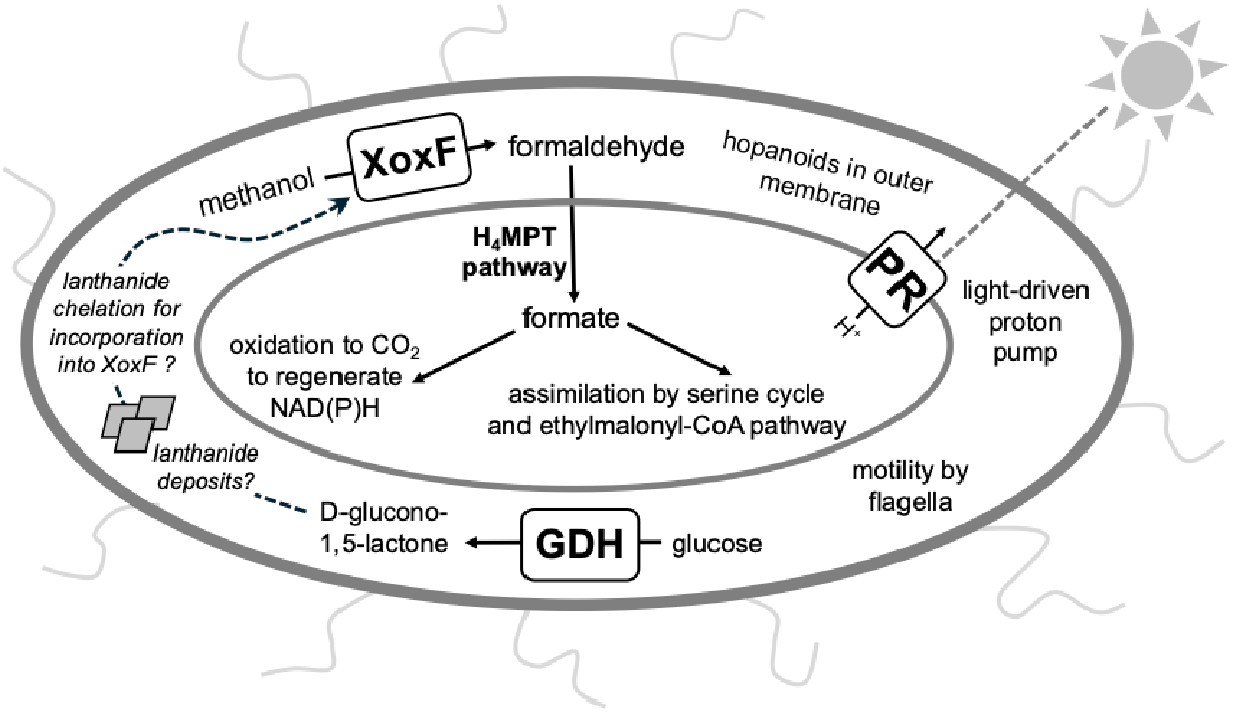


**Figure 3. Schematic of key metabolisms and functions in TMED127/Methylaequorales based on genomic reconstruction**. Three of the most highly transcribed proteins are shown (PQQ-dependent methanol dehydrogenase (XoxF), PQQ-dependent glucose dehydrogenase (GDH), and proteorhopsin (PR)). Question marks represent hypothetical lanthanide deposits and lanthanide chelation by D-glucono-1,5-lactone, which remains unconfirmed.

***TMED127/Methylaequorales are a deep branching alphaproteobacterial order that are widespread in the global oceans.*** We constructed a phylogeny using the conserved protein NADH ubiquinone oxidoreductase subunit L (NuoL) as in Cevallos and Degli Esposti (59). As previously reported (60), the TMED127 order is deep-branching, along with the orders Puniceispirillales, TMED109, and Rickettsiales **(Fig. 4A)**. To date, the TMED127/Methylaequorales order contains only one family (TMED127/Methylaequoraceae) and twelve genera **(Fig. 4A)**. The three genera with highest relative abundance in marine metagenomes (up to ~4% relative abundance each) were TMED13 (0-48° N/S latitude; **Fig. 4B; Table S6)**, GCA-2691245 (*Methylaequorum*; 0-45° N/S latitude; **Fig. 4C; Table S7)**, and SP4073 (16-46° N/S latitude; **Fig. 4D; Table S8).** TMED127/Methylaequorales were not observed at relative abundances of >0.1% above 50° N/S latitude.

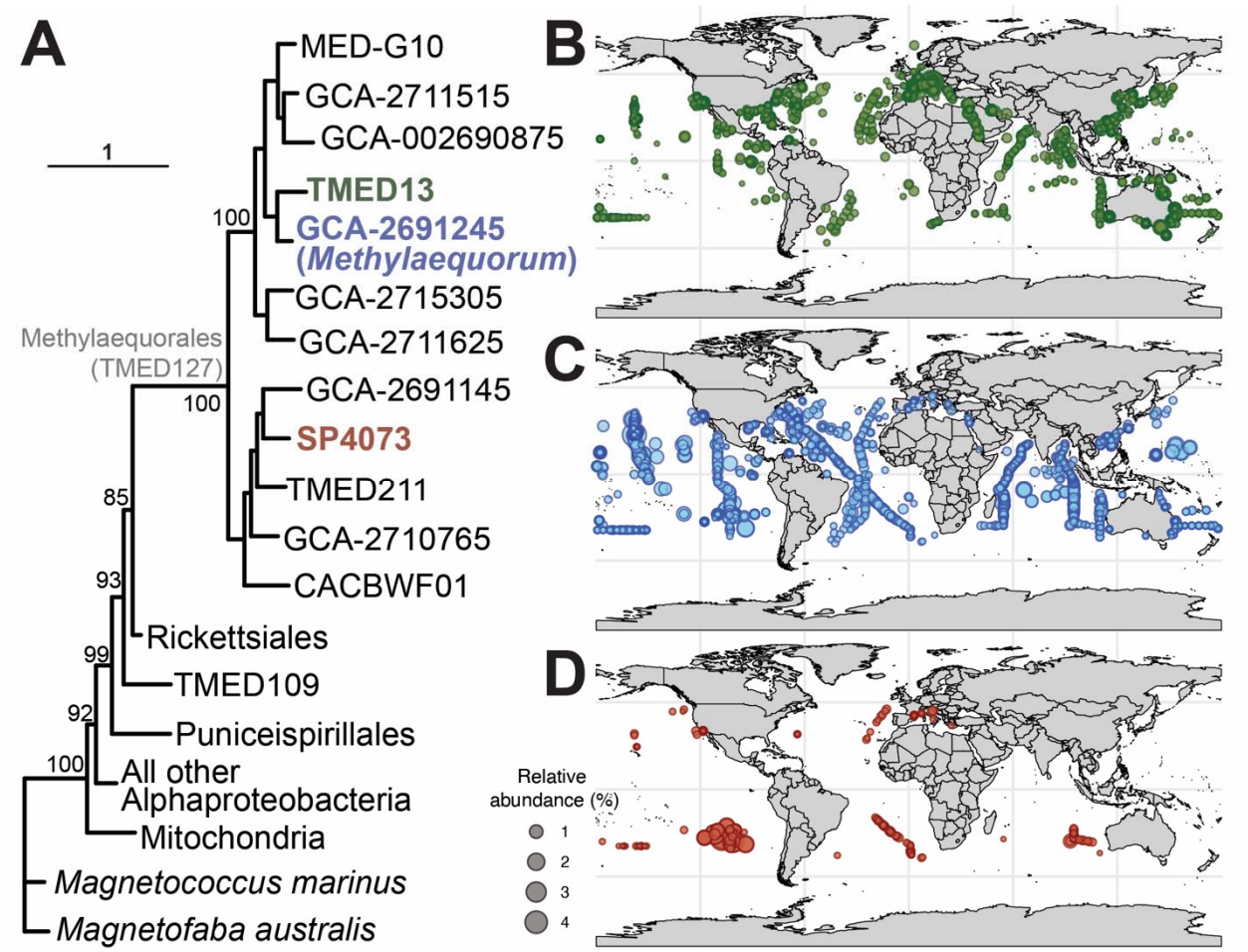


**Figure 4. Alphaproteobacterial phylogeny, geographic distribution, and relative abundance of TMED127/Methylaequorales genera.** (A) Phylogeny was constructed using the alphaproteobacterial phylogenetic marker NADH ubiquinone oxidoreductase subunit L (NuoL). TMED127/Methylaequorales genera are labelled. Scale bar represents substitutions per site. Colors of genera on phylogeny correspond to colors on B-D panels. (B) Relative abundance bubble plot of genus TMED13 overlaid on global map. (C) Relative abundance bubble plot of genus GCA-2691245 (*Methylaequorum*) overlaid on global map. (D) Relative abundance bubble plot of genus SP4073 overlaid on global map.

## Discussion

This study illuminates the identity, metabolism, and diel rhythms of TMED127 (proposed name: Methylaequorales (order); Methylaequoraceae (family)), a deep-branching order of marine alphaproteobacteria (60) that can comprise up to ~10% of metagenomic reads in surface seawater. Although confirmation of their physiology and metabolism will require isolation and

culture experiments, TMED127/Methylaequorales appear to be free-living obligate methylotrophs that are widespread in global oceans, particularly in tropical and subtropical latitudes. This order is highly transcriptionally active, with a diel cycle of *xoxF5* transcription peaking in the late afternoon in surface water of the Sargasso Sea.

The source of methanol to TMED127/Methylaequorales is unknown. It may be produced as a waste product by eukaryotic phytoplankton and/or cyanobacteria, as is known to occur in culture experiments (7, 8), and via photochemical or enzymatic degradation of other organic molecules produced by phytoplankton in surface seawater (9-12). Peak *xoxF5* transcription in the late afternoon suggests that methylotrophy by TMED127/Methylaequorales is subject to temporal niche partitioning (61), and that methanol supply may be highest in the late afternoon. Seawater carbohydrate concentrations are highest in the afternoon, likely due to passive leakage of uncharged molecules during “photosynthetic overflow” from phytoplankton (62). It is possible that similar methanol leakage from phytoplankton also peaks in the afternoon, but further study of methanol production mechanisms in seawater is required.

PQQ-dependent glucose dehydrogenase (GDH), a periplasmic protein that oxidizes D-glucose to D-glucono-1,5-lactone using calcium as a cofactor (63), showed a synchronous transcriptional pattern to *xoxF5* in TMED127/Methylaequorales, rising throughout the day and falling at night. D-glucono-1,5-lactone is a strong metal chelator that can solubilize calcium phosphate minerals (64) and may function as a lanthanide chelator in methylotrophic bacteria (65). Crystalline accumulations of lanthanides are present in the periplasm (65, 66) and cytoplasm (50) of terrestrial alphaproteobacterial methylotrophs. We hypothesize that D-glucono-1,5-lactone production by GDH releases lanthanides from intracellular storage deposits

for incorporation into XoxF **(Fig. 3)**; this hypothesis will require future testing once bacterial isolates are available.

The full complement of lanthanide acquisition and storage pathways in TMED127/Methylaequorales also requires more study. We identified genes encoding the high affinity lanthanide uptake transport system (LutABEFCG; 50), but did not find homologs of genes for "lanthanophore" ligands (67) nor lanthanum storage proteins such as lanmodulin (68) and lanpepsy (69). Given the extremely low (picomolar) lanthanide concentrations in seawater (70, 71), it seems likely that these bacteria have additional lanthanide scavenging strategies, possibly involving one or more of the highly transcribed genes of unknown function.

Our findings suggest that TMED127/Methylaequorales may be the key player in lanthanide-dependent methylotrophy in oligotrophic seawater. More studies are needed to determine whether a diel cycle of methanol production occurs in surface seawater and the quantitative importance of TMED127/Methylaequorales in the global carbon and lanthanide cycles.

## Materials and Methods

**Identifying and quantifying *xoxF* gene transcription in seawater samples.** A python code (GeneSweeper; available at https://github.com/GlassLabGT/Python-scripts) was used to search for all possible product names for the target protein, PQQ-dependent methanol dehydrogenase: ("PQQ-dependent dehydrogenase (methanol/ethanol family)", "methanol dehydrogenase (cytochrome c) subunit 1", "methanol dehydrogenase (cytochrome)", "alcohol dehydrogenase (cytochrome c)", "glucose dehydrogenase", "quinohemoprotein ethanol dehydrogenase", and "quinoprotein glucose dehydrogenase") in CSV files (including gene ID, product name, scaffold

ID, gene sequence length, and read count) for all coastal and marine datasets in Joint Genome Institute's (JGI) Integrated Microbial Genome (IMG) RNASeq Studies database as of May 2025. Only unamended seawater samples were processed; enrichments or laboratory cultures were removed. The total read count of each metatranscriptome was obtained from the JGI IMG RNASeq Studies database. Gene transcription was then converted to reads per kilobase per million mapped reads (RPKM). Amino acid sequences were obtained from reference metagenomes using the JGI IMG "Find Genes" function with the Gene ID as input. Each amino acid sequence was then queried against the NCBI nr database by BLASTP search (May 2025). Only full-length gene sequences were kept for further processing. The top NCBI hit was matched to its GTDB taxonomy (release 10-RS226) by searching GTDB (46) for the GCA assembly of the SAG/MAG.

**XoxF phylogeny.** Sequences ($n$ = 50; 550 gap-free sites) were aligned using the MAFFT online server with the L-INS-i method (72). A maximum likelihood phylogeny with 1000 bootstraps was constructed in W-IQ-tree (73, 74) using the LG+F+I+G4 model based on ModelFinder results (75) with ultrafast 1000 bootstraps (73). The phylogeny was visualized in iTOL (76). The alignment fasta file (XoxF_alignment.fasta) is available as a supplemental data set.

**Transcription of *xoxF* in Eastern Tropical North Pacific oxygen minimum zone**. Magic-Basic Local Alignment Search Tool (Magic-BLAST) (77) was used with default parameters to search ETNP ODZ metatranscriptomes (PRJNA727903; 47) for *xoxF* genes from UBA11136 MAGs using DNA sequence of *xoxF5* from Alphaproteobacteria bacterium isolate

ETNP15_MAG_21 (MDP6304722) as the query. Read hits were normalized to reads per kilobase million (RPKM).

**TMED127 SAG/MAG analysis and mapping to metatranscriptomes.** All SAG/MAGs in the Alphaproteobacteria order TMED127 in GTDB release 10-RS226 were collected into a BV-BRC genome group, which was used to search for product names via "Proteins" tab and for metabolic pathways via "Pathways" tab (78). The TMED127 SAG AG-892-F10 (estimated 90% completeness; 0.01% contamination; 53) was chosen for further study because it was the most complete SAG/MAG from the genus GCA-2691245, which contained the most abundant *xoxF5* transcripts in surface seawater (see text). Additional analysis was performed in KBase (79). SAG AG-892-F10 (NCBI WGS Project CACMWI01; genome assembly GCA_902617375.1) and *Methylorubrum extorquens* AM1 (NCBI Reference Sequence NC_012808.1) were imported into KBase, and the KBase program "Compare Two Proteomes" was used to find homologs. RNA-Seq data (JGI GOLD Study ID Gs0161320; **Table S4**) were imported into KBase and aligned to SAG AG-892-F10 using the Bowtie2 app (80). The aligned RNA-Seq data was then assembled into a set of transcripts quantified by transcripts per million (TPM) using the StringTie v.2.1.5 (81) app.

**Alphaproteobacteria NuoL phylogeny.** A phylogeny of alphaproteobacterial NADH ubiquinone oxidoreductase subunit L (NuoL) and mitochondrial ND5 marker proteins ($n$ = 146; 510 gap-free sites) were aligned with MAFFT online server with the L-INS-i method (72). Sequences from two species of c__Magnetococcia were used as the outgroup. A maximum likelihood phylogeny with 1000 bootstraps was constructed in W-IQ-tree (73, 74) using the

LG+F+I+G4 model based on ModelFinder results (75) with ultrafast 1000 bootstraps (73). The phylogeny was visualized in iTOL (76). The alignment fasta file (NuoL _alignment) is available as a supplemental data set.

**Gene neighborhood.** The methylotrophy gene neighborhood was generated using the EFI Gene Neighborhood Tool (48) with single sequence BLAST of the UniProt database with NCBI accession GIR25668 as the query.

**Distribution and relative abundance of TMED127 genera.** The twelve TMED127 genera were individually searched for using Sandpiper (82) was searched for used to obtain csv files with relative abundance, latitude, and longitude data. Samples with <0.1% relative abundance of each TMED127 genus were removed. Global maps were overlaid with relative abundance data for the three most abundant genera in R using gglot2 (83).

**Data Availability**. The KBase bioinformatic pipeline is available at https://narrative.kbase.us/narrative/214786. SAG AG-892-F10 is available as NCBI BioSample SAMEA6069714 (SRA: ERS3870829; GCA_902617375.1). RNA-Seq data for the BATS timeseries is available as JGI GOLD Study ID Gs0161320. The TMED127 BV-BRC genome group is available at https://www.bv-brc.org/workspace/jbglass1@patricbrc.org/TMED127%20genomes. The newly proposed names have been submitted to the SeqCode Registry as accession seqco.de/r:_v7atfaf.

**Acknowledgments**

We thank Naomi Gilbert, Steven Wilhelm, Matthew Sullivan, and David Walsh for providing access to sequences and metadata. We thank Ann Pearson, Paul Carini, and Steven Wilhelm for helpful discussions. We thank William Whitman and Luis-Miguel Rodríguez Rojas for curation assistance with submission to SeqCode Registry.

## References


1. Chistoserdova L, Kalyuzhnaya MG. 2018. Current trends in methylotrophy. Trends Microbiol 26:703-714.

2. Chistoserdova L, Kalyuzhnaya MG, Lidstrom ME. 2009. The expanding world of methylotrophic metabolism. Annu Rev Microbiol 63:477-99.

3. Keltjens JT, Pol A, Reimann J, Op den Camp HJ. 2014. PQQ-dependent methanol dehydrogenases: rare-earth elements make a difference. Appl Microbiol Biotechnol 98:6163-83.

4. Chistoserdova L. 2011. Modularity of methylotrophy, revisited. Environ Microbiol 13:2603-2622.

5. Dorokhov YL, Sheshukova EV, Komarova TV. 2018. Methanol in plant life. Front Plant Sci 9:1623.

6. Zhang C, Wang M-Y, Khan N, Tan L-L, Yang S. 2021. Potentials, utilization, and bioengineering of plant growth-promoting *Methylobacterium* for sustainable agriculture. Sustainability 13:3941.

7. Mincer TJ, Aicher AC. 2016. Methanol production by a broad phylogenetic array of marine phytoplankton. PLoS One 11:e0150820.

8. Halsey KH, Giovannoni SJ, Graus M, Zhao Y, Landry Z, Thrash JC, Vergin KL, de Gouw J. 2017. Biological cycling of volatile organic carbon by phytoplankton and bacterioplankton. Limnol Oceanogr 62:2650-2661.

9. Ossola R, Gruseck R, Houska J, Manfrin A, Vallieres M, McNeill K. 2022. Photochemical production of carbon monoxide from dissolved organic matter: role of lignin methoxyarene functional groups. Environ Sci Technol 56:13449-13460.

10. Khan MAH, Cooke MC, Utembe SR, Xiao P, Derwent RG, Jenkin ME, Archibald AT, Maxwell P, Morris WC, South N, Percival CJ, Shallcross DE. 2014. Reassessing the photochemical production of methanol from peroxy radical self and cross reactions using the STOCHEM-CRI global chemistry and transport model. Atmospheric Environment 99:77-84.

11. McCarren J, Becker JW, Repeta DJ, Shi Y, Young CR, Malmstrom RR, Chisholm SW, DeLong EF. 2010. Microbial community transcriptomes reveal microbes and metabolic pathways associated with dissolved organic matter turnover in the sea. Proceedings of the National Academy of Sciences 107:16420–16427.

12. Hehemann JH, Truong LV, Unfried F, Welsch N, Kabisch J, Heiden SE, Junker S, Becher D, Thurmer A, Daniel R, Amann R, Schweder T. 2017. Aquatic adaptation of a laterally acquired pectin degradation pathway in marine gammaproteobacteria. Environ Microbiol 19:2320-2333.

13. Kaur A, Hernandez-Fernaud JR, Aguilo-Ferretjans MDM, Wellington EM, Christie-Oleza JA. 2018. 100 days of marine *Synechococcus-Ruegeria pomeroyi* interaction: A detailed analysis of the exoproteome. Environ Microbiol 20:785-799.

14. Bates KH, Jacob DJ, Wang S, Hornbrook RS, Apel EC, Kim MJ, Millet DB, Wells KC, Chen X, Brewer JF, Ray EA, Commane R, Diskin GS, Wofsy SC. 2021. The global budget of atmospheric methanol: new constraints on secondary, oceanic, and terrestrial sources. Journal of Geophysical Research: Atmospheres 126:e2020JD033439.

15. Yang M, Nightingale PD, Beale R, Liss PS, Blomquist B, Fairall C. 2013. Atmospheric deposition of methanol over the Atlantic Ocean. Proceedings of the National Academy of Sciences 110:20034–20039

16. Carpenter LJ, Lewis AC, Hopkins JR, Read KA, Longley ID, Gallagher MW. 2004. Uptake of methanol to the North Atlantic Ocean surface. Global Biogeochemical Cycles 18.

17. Dixon JL, Beale R, Nightingale PD. 2011. Rapid biological oxidation of methanol in the tropical Atlantic: significance as a microbial carbon source. Biogeosciences 8:2707-2716.

18. Dixon JL, Beale R, Nightingale PD. 2011. Microbial methanol uptake in northeast Atlantic waters. ISME J 5:704-16.

19. Zhou Z, Zhuang GC, Mao SH, Liu J, Li XJ, Liu Q, Song GD, Zhang HH, Chen Z, Montgomery A, Joye S, Yang GP. 2023. Methanol concentrations and biological methanol consumption in the Northwest Pacific Ocean. Geophys Res Lett 50:e2022GL101605.

20. Dixon JL, Nightingale PD. 2012. Fine-scale variability in methanol uptake and oxidation: from the microlayer to 1000 m. Biogeosciences 9:2961-2972.

21. Dixon JL, Sargeant S, Nightingale PD, Colin Murrell J. 2013. Gradients in microbial methanol uptake: productive coastal upwelling waters to oligotrophic gyres in the Atlantic Ocean. ISME J 7:568-80.

22. Voutsinos MY, Banfield JF, McClelland HO. 2025. Extensive and diverse lanthanide-dependent metabolism in the ocean. ISME J 19:wraf057.

23. Huang J, Yu Z, Chistoserdova L. 2018. Lanthanide-dependent methanol dehydrogenases of XoxF4 and XoxF5 clades are differentially distributed among methylotrophic bacteria and they reveal different biochemical properties. Front Microbiol 9:1366.

24. Huang J, Yu Z, Groom J, Cheng J-F, Tarver A, Yoshikuni Y, Chistoserdova L. 2019. Rare earth element alcohol dehydrogenases widely occur among globally distributed, numerically abundant and environmentally important microbes. ISME J 13:2005-2017.

25. Shiller AM, Chan EW, Joung DJ, Redmond MC, Kessler JD. 2017. Light rare earth element depletion during Deepwater Horizon blowout methanotrophy. Sci Rep 7:10389.

26. Hara Y, Obata H, Doi T, Hongo Y, Gamo T, Takeda S, Tsuda A. 2009. Rare earth elements in seawater during an iron-induced phytoplankton bloom of the western subarctic Pacific (SEEDS-II). Deep Sea Research Part II: Topical Studies in Oceanography 56:2839-2851.

27. Meyer ACS, Grundle D, Cullen JT. 2021. Selective uptake of rare earth elements in marine systems as an indicator of and control on aerobic bacterial methanotrophy. Earth and Planetary Science Letters 558:116756.

28. Giovannoni SJ, Hayakawa DH, Tripp HJ, Stingl U, Givan SA, Cho JC, Oh HM, Kitner JB, Vergin KL, Rappe MS. 2008. The small genome of an abundant coastal ocean methylotroph. Environ Microbiol 10:1771-82.

29. Sowell SM, Abraham PE, Shah M, Verberkmoes NC, Smith DP, Barofsky DF, Giovannoni SJ. 2011. Environmental proteomics of microbial plankton in a highly productive coastal upwelling system. ISME J 5:856-65.

30. Rappé MS, Kemp PF, Giovannoni SJ. 2003. Phylogenetic diversity of marine coastal picoplankton 16S rRNA genes cloned from the continental shelf off Cape Hatteras, North Carolina. Limnol Oceanogr 42:811-826.

31. Ramachandran A, Walsh DA. 2015. Investigation of XoxF methanol dehydrogenases reveals new methylotrophic bacteria in pelagic marine and freshwater ecosystems. FEMS Microbiol Ecol 91:fiv105.

32. Taubert M, Grob C, Howat AM, Burns OJ, Dixon JL, Chen Y, Murrell JC. 2015. XoxF encoding an alternative methanol dehydrogenase is widespread in coastal marine environments. Environ Microbiol 17:3937-3948.

33. Georges AA, El-Swais H, Craig SE, Li WK, Walsh DA. 2014. Metaproteomic analysis of a winter to spring succession in coastal northwest Atlantic Ocean microbial plankton. ISME J 8:1301-13.

34. Morris RM, Longnecker K, Giovannoni SJ. 2006. Pirellula and OM43 are among the dominant lineages identified in an Oregon coast diatom bloom. Environ Microbiol 8:1361-70.

35. Neufeld JD, Schafer H, Cox MJ, Boden R, McDonald IR, Murrell JC. 2007. Stable-isotope probing implicates Methylophaga spp and novel Gammaproteobacteria in marine methanol and methylamine metabolism. ISME J 1:480-91.

36. Janvier M. 1985. *Methylophaga marina* gen. nov. sp. nov. and *Methylophaga thalassica* sp. nov., marine methylotrophs. Int J System Bacteriol 35:131-139.

37. Grob C, Taubert M, Howat AM, Burns OJ, Dixon JL, Richnow HH, Jehmlich N, von Bergen M, Chen Y, Murrell JC. 2015. Combining metagenomics with metaproteomics and stable isotope probing reveals metabolic pathways used by a naturally occurring marine methylotroph. Environ Microbiol 17:4007-18.

38. Francis B, Urich T, Mikolasch A, Teeling H, Amann R. 2021. North Sea spring bloom-associated Gammaproteobacteria fill diverse heterotrophic niches. Environ Microbiome 16:15.

39. Cavaco MA, Bhatia MP, Hawley AK, Torres-Beltrán M, Johnson WM, Longnecker K, Konwar K, Kujawinski EB, Hallam SJ. 2022. Pathway-centric analysis of microbial metabolic potential and expression along nutrient and energy gradients in the Western Atlantic Ocean. Front Mar Sci 9.

40. Hanson BT, Hewson I, Madsen EL. 2014. Metaproteomic survey of six aquatic habitats: discovering the identities of microbial populations active in biogeochemical cycling. Microb Ecol 67:520-39.

41. Zhou Z, Tran PQ, Kieft K, Anantharaman K. 2020. Genome diversification in globally distributed novel marine Proteobacteria is linked to environmental adaptation. ISME J 14:2060-2077.

42. Chen IA, Chu K, Palaniappan K, Ratner A, Huang J, Huntemann M, Hajek P, Ritter SJ, Webb C, Wu D, Varghese NJ, Reddy TBK, Mukherjee S, Ovchinnikova G, Nolan M, Seshadri R, Roux S, Visel A, Woyke T, Eloe-Fadrosh EA, Kyrpides NC, Ivanova NN. 2023. The IMG/M data management and analysis system v.7: content updates and new features. Nucleic Acids Res 51:D723-D732.

43. Gilbert NE, Muratore D, Shopen Gochev C, LeCleir GR, Cagle SM, Pound HL, Sun CL, Carillo A, Ndlovu KS, Maidanik I, Coenen AR, Chittick L, DeBruyn JM, Buchan A, Lindell D, Sullivan MB, Weitz JS, Wilhelm SW. 2025. Seasonal enhancement of the viral shunt catalyzes a subsurface oxygen maximum in the Sargasso Sea. BioRxiv doi:10.1101/2025.01.23.634377.

44. Muratore D, Gilbert NE, LeCleir GR, Wilhelm SW, Weitz JS. 2025. Diel partitioning in microbial phosphorus acquisition in the Sargasso Sea. Proc Natl Acad Sci U S A 122:e2410268122.

45. Gilbert NE, LeCleir GR, Pound HL, Strzepek RF, Ellwood MJ, Twining BS, Roux S, Boyd PW, Wilhelm SW. 2023. Giant virus infection signatures are modulated by euphotic zone depth strata and iron regimes of the subantarctic Southern Ocean. mSystems 8:1-17.

46. Parks DH, Chuvochina M, Rinke C, Mussig AJ, Chaumeil PA, Hugenholtz P. 2022. GTDB: an ongoing census of bacterial and archaeal diversity through a phylogenetically consistent, rank normalized and complete genome-based taxonomy. Nucleic Acids Res 50:D785-D794.

47. Mattes TE, Burke S, Rocap G, Morris RM. 2022. Two metatranscriptomic profiles through low-dissolved-oxygen waters (DO, 0 to 33 µM) in the Eastern Tropical North Pacific Ocean. Microbiol Resour Announc 11:e01201-21.

48. Elbon CE, Stewart FJ, Glass JB. 2024. Novel Alphaproteobacteria transcribe genes for nitric oxide transformation at high levels in a marine oxygen-deficient zone. Appl Environ Microbiol 90:02099-23.

49. Pyne P, Alam M, Rameez MJ, Mandal S, Sar A, Mondal N, Debnath U, Mathew B, Misra AK, Mandal AK, Ghosh W. 2018. Homologs from sulfur oxidation (Sox) and methanol dehydrogenation (Xox) enzyme systems collaborate to give rise to a novel pathway of chemolithotrophic tetrathionate oxidation. Mol Microbiol 109:169-191.

50. Roszczenko-Jasińska P, Vu HN, Subuyuj GA, Crisostomo RV, Cai J, Lien NF, Clippard EJ, Ayala EM, Ngo RT, Yarza F, Wingett JP, Raghuraman C, Hoeber CA, Martinez-Gomez NC, Skovran E. 2020. Gene products and processes contributing to lanthanide homeostasis and methanol metabolism in *Methylorubrum extorquens* AM1. Sci Rep 10:1-15.

51. Bradley AS, Pearson A, Sáenz JP, Marx CJ. 2010. Adenosylhopane: The first intermediate in hopanoid side chain biosynthesis. Organic Geochemistry 41:1075-1081.

52. Saenz JP, Grosser D, Bradley AS, Lagny TJ, Lavrynenko O, Broda M, Simons K. 2015. Hopanoids as functional analogues of cholesterol in bacterial membranes. Proc Natl Acad Sci U S A 112:11971-6.

53. Pachiadaki MG, Brown JM, Brown J, Bezuidt O, Berube PM, Biller SJ, Poulton NJ, Burkart MD, La Clair JJ, Chisholm SW, Stepanauskas R. 2019. Charting the complexity of the marine microbiome through single-cell genomics. Cell 179:1623-1635 e11.

54. Smejkalova H, Erb TJ, Fuchs G. 2010. Methanol assimilation in *Methylobacterium extorquens* AM1: demonstration of all enzymes and their regulation. PLoS One 5:e13001.

55. Chistoserdova L, Chen SW, Lapidus A, Lidstrom ME. 2003. Methylotrophy in *Methylobacterium extorquens* AM1 from a genomic point of view. J Bacteriol 185:2980-7.

56. Crowther GJ, Kosaly G, Lidstrom ME. 2008. Formate as the main branch point for methylotrophic metabolism in *Methylobacterium extorquens* AM1. J Bacteriol 190:5057-62.

57. Laukel M, Chistoserdova L, Lidstrom ME, Vorholt JA. 2003. The tungsten-containing formate dehydrogenase from *Methylobacterium extorquens* AM1: purification and properties. Eur J Biochem 270:325-33.

58. Wood AP, Aurikko JP, Kelly DP. 2004. A challenge for 21st century molecular biology and biochemistry: what are the causes of obligate autotrophy and methanotrophy? FEMS Microbiol Rev 28:335-52.

59. Cevallos MA, Degli Esposti M. 2022. New Alphaproteobacteria thrive in the depths of the ocean with oxygen gradient. Microorganisms 10:455.

60. Geiger O, Sanchez-Flores A, Padilla-Gomez J, Degli Esposti M. 2023. Multiple approaches of cellular metabolism define the bacterial ancestry of mitochondria. Sci Adv 9:eadh0066.

61. Muratore D, Boysen AK, Harke MJ, Becker KW, Casey JR, Coesel SN, Mende DR, Wilson ST, Aylward FO, Eppley JM, Vislova A, Peng S, Rodriguez-Gonzalez RA, Beckett SJ, Virginia Armbrust E, DeLong EF, Karl DM, White AE, Zehr JP, Van Mooy BAS, Dyhrman ST, Ingalls AE, Weitz JS. 2022. Complex marine microbial communities partition metabolism of scarce resources over the diel cycle. Nat Ecol Evol 6:218-229.

62. Barthelmess T, Cristi A, Deppeler S, Safi K, Sellegri K, Law CS, Engel A. 2025. Pronounced diel cycling of dissolved carbohydrates and amino acids in the surface ocean and across diverse regimes. Environ Sci Technol 59:419-429.

63. Southall SM, Doel JJ, Richardson DJ, Oubrie A. 2006. Soluble aldose sugar dehydrogenase from Escherichia coli: a highly exposed active site conferring broad substrate specificity. J Biol Chem 281:30650-9.

64. Sashidhar B, Podile AR. 2010. Mineral phosphate solubilization by rhizosphere bacteria and scope for manipulation of the direct oxidation pathway involving glucose dehydrogenase. J Appl Microbiol 109:1-12.

65. Gorniak L, Bechwar J, Westermann M, Steiniger F, Wegner C-E. 2023. Different lanthanide elements induce strong gene expression changes in a lanthanide-accumulating methylotroph. Microbiology Spectrum 11:e00867-23.

66. Wegner CE, Westermann M, Steiniger F, Gorniak L, Budhraja R, Adrian L, Kusel K. 2021. Extracellular and intracellular lanthanide accumulation in the methylotrophic Beijerinckiaceae bacterium RH AL1. Appl Environ Microbiol 87:e0314420.

67. Zytnick AM, Gutenthaler-Tietze SM, Aron AT, Reitz ZL, Phi MT, Good NM, Petras D, Daumann LJ, Martinez-Gomez NC. 2024. Identification and characterization of a small-molecule metallophore involved in lanthanide metabolism. Proc Natl Acad Sci U S A 121:e2322096121.

68. Cotruvo JA, Jr., Featherston ER, Mattocks JA, Ho JV, Laremore TN. 2018. Lanmodulin: a highly selective lanthanide-binding protein from a lanthanide-utilizing bacterium. J Am Chem Soc 140:15056-15061.

69. Hemmann JL, Keller P, Hemmerle L, Vonderach T, Ochsner AM, Bortfeld-Miller M, Gunther D, Vorholt JA. 2023. Lanpepsy is a novel lanthanide-binding protein involved in the lanthanide response of the obligate methylotroph *Methylobacillus flagellatus*. J Biol Chem 299:102940.

70. Hatje V, Schijf J, Johannesson KH, Andrade R, Caetano M, Brito P, Haley BA, Lagarde M, Jeandel C. 2024. The global biogeochemical cycle of the rare earth elements. Global Biogeochemical Cycles 38.

71. Noack CW, Dzombak DA, Karamalidis AK. 2014. Rare earth element distributions and trends in natural waters with a focus on groundwater. Environ Sci Technol 48:4317-26.

72. Katoh K, Rozewicki J, Yamada KD. 2019. MAFFT online service: multiple sequence alignment, interactive sequence choice and visualization. Brief Bioinform 20:1160-1166.

73. Trifinopoulos J, Nguyen LT, von Haeseler A, Minh BQ. 2016. W-IQ-TREE: a fast online phylogenetic tool for maximum likelihood analysis. Nucleic Acids Res 44:W232-5.

74. Nguyen LT, Schmidt HA, von Haeseler A, Minh BQ. 2015. IQ-TREE: a fast and effective stochastic algorithm for estimating maximum-likelihood phylogenies. Mol Biol Evol 32:268-74.

75. Kalyaanamoorthy S, Minh BQ, Wong TKF, von Haeseler A, Jermiin LS. 2017. ModelFinder: fast model selection for accurate phylogenetic estimates. Nat Methods 14:587-589.

76. Letunic I, Bork P. 2024. Interactive Tree of Life (iTOL) v6: recent updates to the phylogenetic tree display and annotation tool. Nucleic Acids Res 52:W78-W82.

77. Boratyn GM, Thierry-Mieg J, Thierry-Mieg D, Busby B, Madden TL. 2019. Magic-BLAST, an accurate RNA-seq aligner for long and short reads. BMC Bioinf 20:405.

78. Olson RD, Assaf R, Brettin T, Conrad N, Cucinell C, Davis JJ, Dempsey DM, Dickerman A, Dietrich EM, Kenyon RW, Kuscuoglu M, Lefkowitz EJ, Lu J, Machi D, Macken C, Mao C, Niewiadomska A, Nguyen M, Olsen GJ, Overbeek JC, Parrello B, Parrello V, Porter JS, Pusch GD, Shukla M, Singh I, Stewart L, Tan G, Thomas C, VanOeffelen M, Vonstein V, Wallace ZS, Warren AS, Wattam AR, Xia F, Yoo H, Zhang Y, Zmasek CM, Scheuermann RH, Stevens RL. 2023. Introducing the Bacterial and Viral Bioinformatics Resource Center (BV-BRC): a resource combining PATRIC, IRD and ViPR. Nucleic Acids Res 51:D678-D689.

79. Arkin AP, Cottingham RW, Henry CS, Harris NL, Stevens RL, Maslov S, Dehal P, Ware D, Perez F, Canon S, Sneddon MW, Henderson ML, Riehl WJ, Murphy-Olson D, Chan SY, Kamimura RT, Kumari S, Drake MM, Brettin TS, Glass EM, Chivian D, Gunter D, Weston DJ, Allen BH, Baumohl J, Best AA, Bowen B, Brenner SE, Bun CC, Chandonia JM, Chia JM, Colasanti R, Conrad N, Davis JJ, Davison BH, DeJongh M, Devoid S, Dietrich E, Dubchak I, Edirisinghe JN, Fang G, Faria JP, Frybarger PM, Gerlach W, Gerstein M, Greiner A, Gurtowski J, Haun HL, He F, Jain R, et al. 2018. KBase: The United States Department of Energy Systems Biology Knowledgebase. Nat Biotechnol 36:566-569.

80. Langmead B, Salzberg SL. 2012. Fast gapped-read alignment with Bowtie 2. Nat Methods 9:357-9.

81. Pertea M, Pertea GM, Antonescu CM, Chang TC, Mendell JT, Salzberg SL. 2015. StringTie enables improved reconstruction of a transcriptome from RNA-seq reads. Nat Biotechnol 33:290-5.

82. Woodcroft BJ, Aroney STN, Zhao R, Cunningham M, Mitchell JAM, Blackall L, Tyson GW. 2024. SingleM and Sandpiper: Robust microbial taxonomic profiles from metagenomic data. BioRxiv doi:10.1101/2024.01.30.578060:https://doi.org/10.1101/2024.01.30.578060.

83. Wickham H. 2016. Programming with ggplot2, p 241-253, Ggplot2: elegant graphics for data analysis. Springer.

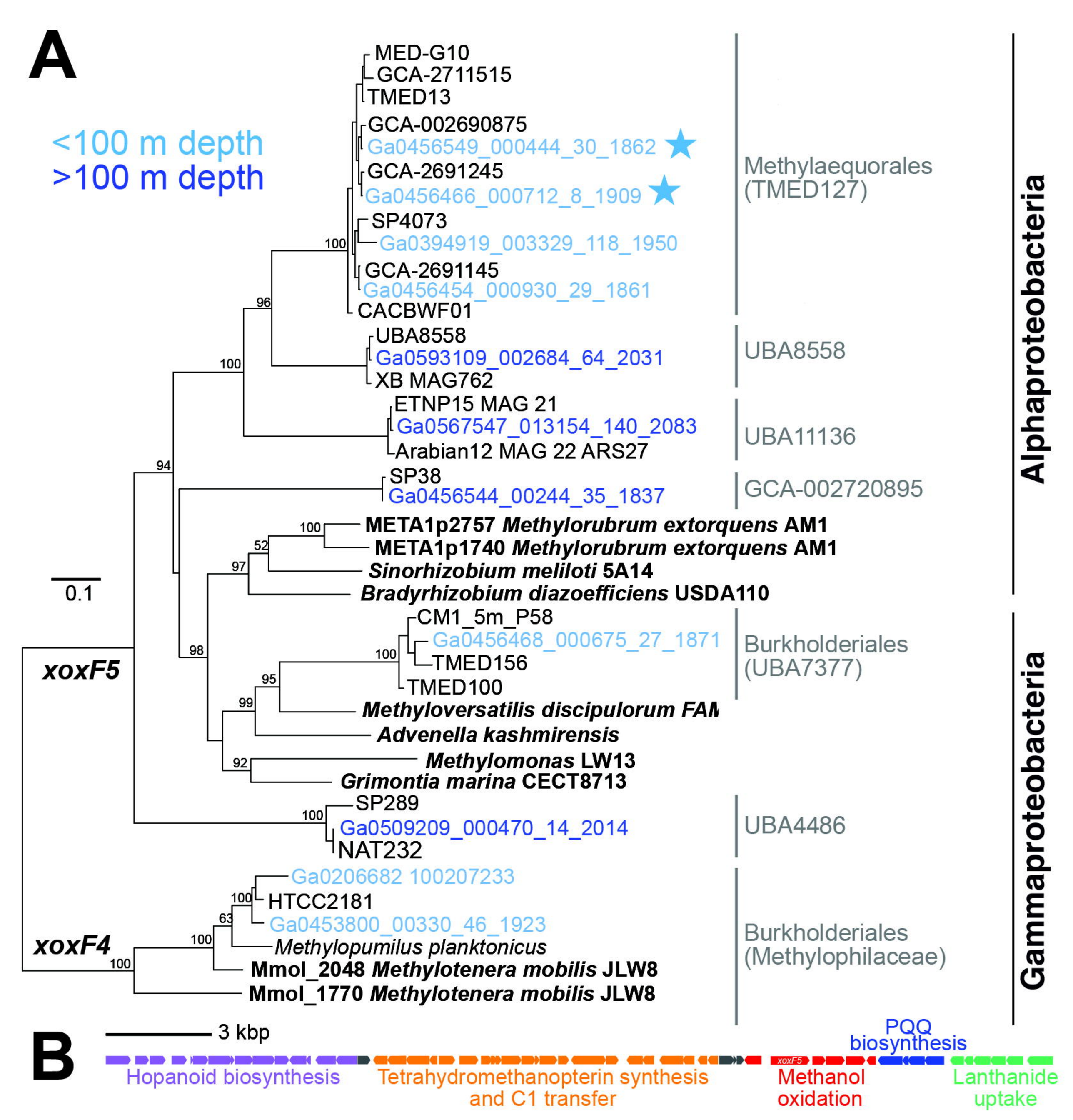
A
<100 m depth
>100 m depth
MED-G10
GCA-2711515
TMED13
GCA-002690875
Ga0456549_000444_30_1862
GCA-2691245
Ga0456466_000712_8_1909
SP4073
Ga0394919_003329_118_1950
GCA-2691145
Ga0456454_000930_29_1861
CACBWF01
UBA8558
Ga0593109_002684_64_2031
XB MAG762
ETNP15 MAG 21
Ga0567547_013154_140_2083
Arabian12 MAG 22 ARS27
SP38
Ga0456544_00244_35_1837
META1p2757 Methylorubrum extorquens AM1
META1p1740 Methylorubrum extorquens AM1
Sinorhizobium meliloti 5A14
Bradyrhizobium diazoefficiens USDA110
CM1_5m_P58
Ga0456468_000675_27_1871
TMED156
TMED100
Methyloversatilis discipulorum FAM
Advenella kashmirensis
Methylomonas LW13
Grimontia marina CECT8713
SP289
Ga0509209_000470_14_2014
NAT232
Ga0206682 100207233
HTCC2181
Ga0453800_00330_46_1923
Methylopumilus planktonicus
Mmol_2048 Methylotenera mobilis JLW8
Mmol_1770 Methylotenera mobilis JLW8
0.1
xoxF5
xoxF4
Methylaequorales (TMED127)
UBA8558
UBA11136
GCA-002720895
Burkholderiales (UBA7377)
UBA4486
Burkholderiales (Methylophilaceae)
Alphaproteobacteria
Gammaproteobacteria
B
3 kbp
Hopanoid biosynthesis
Tetrahydromethanopterin synthesis and C1 transfer
xoxF5
Methanol oxidation
PQQ biosynthesis
Lanthanide uptake

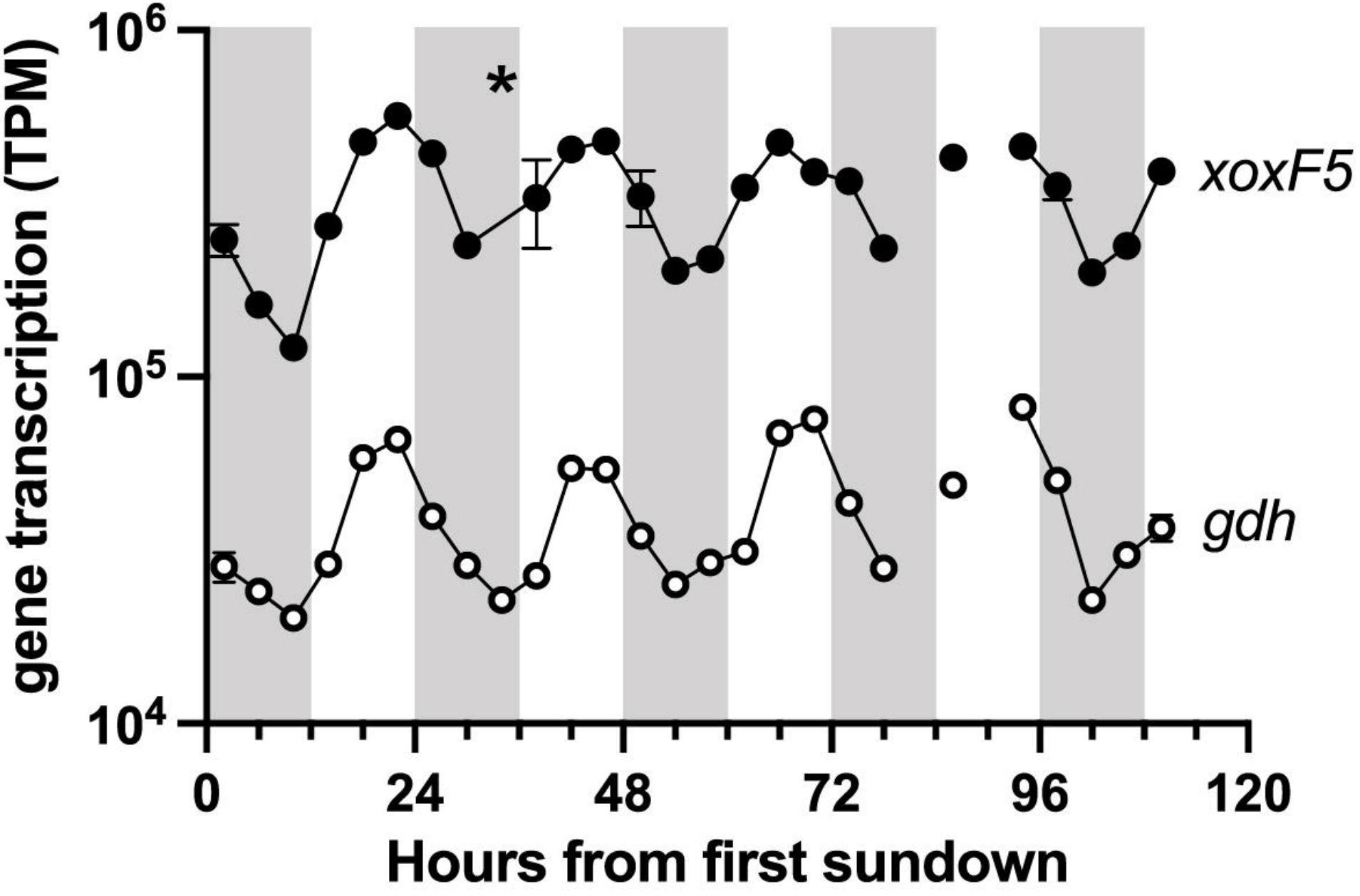
gene transcription (TPM)
$10^6$
$10^5$
$10^4$
*
xoxF5
gdh
0
24
48
72
96
120
Hours from first sundown

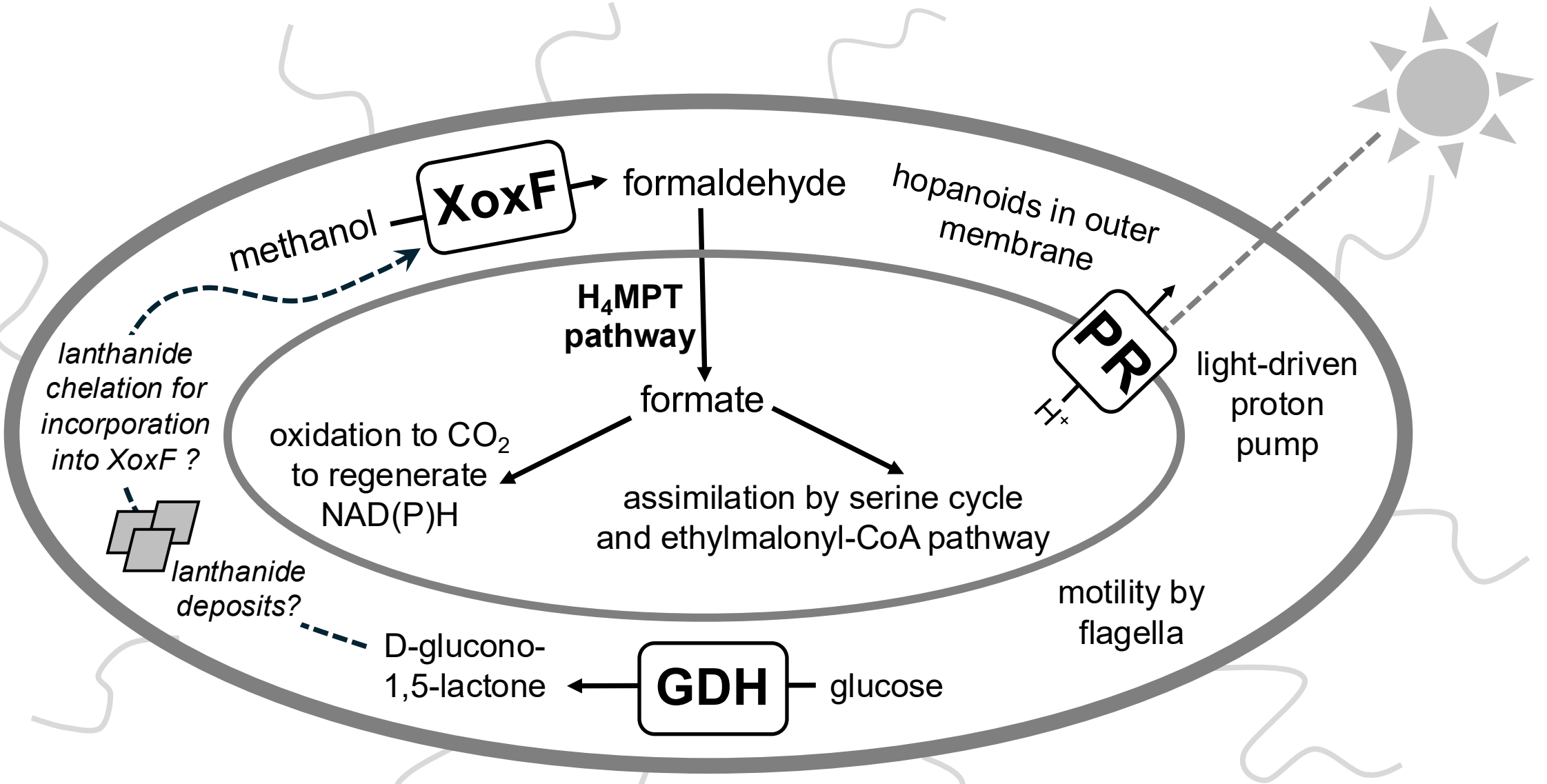
methanol
XoxF
formaldehyde
hopanoids in outer membrane
H4MPT pathway
formate
PR
H+
light-driven proton pump
lanthanide chelation for incorporation into XoxF ?
oxidation to CO2 to regenerate NAD(P)H
assimilation by serine cycle and ethylmalonyl-CoA pathway
lanthanide deposits?
motility by flagella
D-glucono-1,5-lactone
GDH
glucose

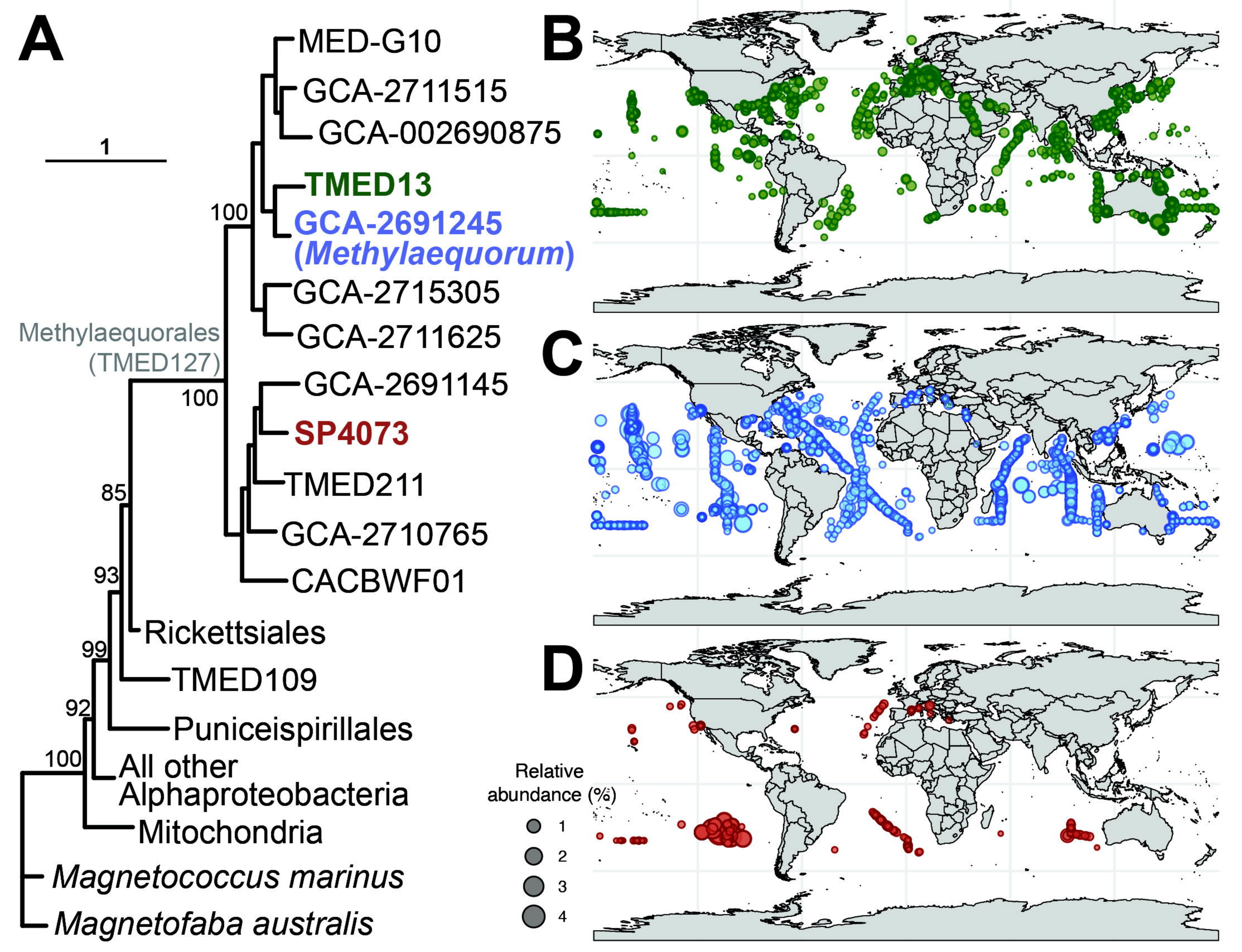
A
B
C
D
1
MED-G10
GCA-2711515
GCA-002690875
TMED13
GCA-2691245
(Methylaequorum)
GCA-2715305
GCA-2711625
GCA-2691145
SP4073
TMED211
GCA-2710765
CACBWF01
Rickettsiales
TMED109
Puniceispirillales
All other
Alphaproteobacteria
Mitochondria
Magnetococcus marinus
Magnetofaba australis
Methylaequorales
(TMED127)
100
100
85
93
99
92
100
Relative
abundance (%)
1
2
3
4